Tomographic reconstruction of internal instability in a field-reversed configuration

T. Kiguchi, T. Asai, N. Yamamoto, S. Hiromori, T. Okano, T. Takahashi,
T. Takahashi[1], Y. Nogi and S. Inagaki[2]

College of science and technology, Nihon University, Tokyo, Japan
1) Faculty of Engineering, Gunma University, Kiryu, Japan
2) National Institute for Fusion Science, Toki, Japan

Introduction

Toroidal mode deformation of the plasma cross section, especially n=2 mode, is well known as a factor which limits the confinement and destroy the configuration of FRC plasma.
In this report, the time evolutions of the each toroidal mode deformation are investigated by an optical measur-ement (azimuthal array and Computer tomography).
In the past experiment with tomographic reconstruction technique, time evolution of the internal structure of FRC has been investigated. These results indicate that the FRC plasma has an internal deformation, which has different phase from the deformation of separatrix surface. These two different toroidal deformation are difficult to be observed by spatially integrated methods, for example, interferometer, end-on camera and so on.
Therefore, in this work, detailed features of this internal behavior have been investigated by a newly improved tomographic reconstruction method.

Experimental device

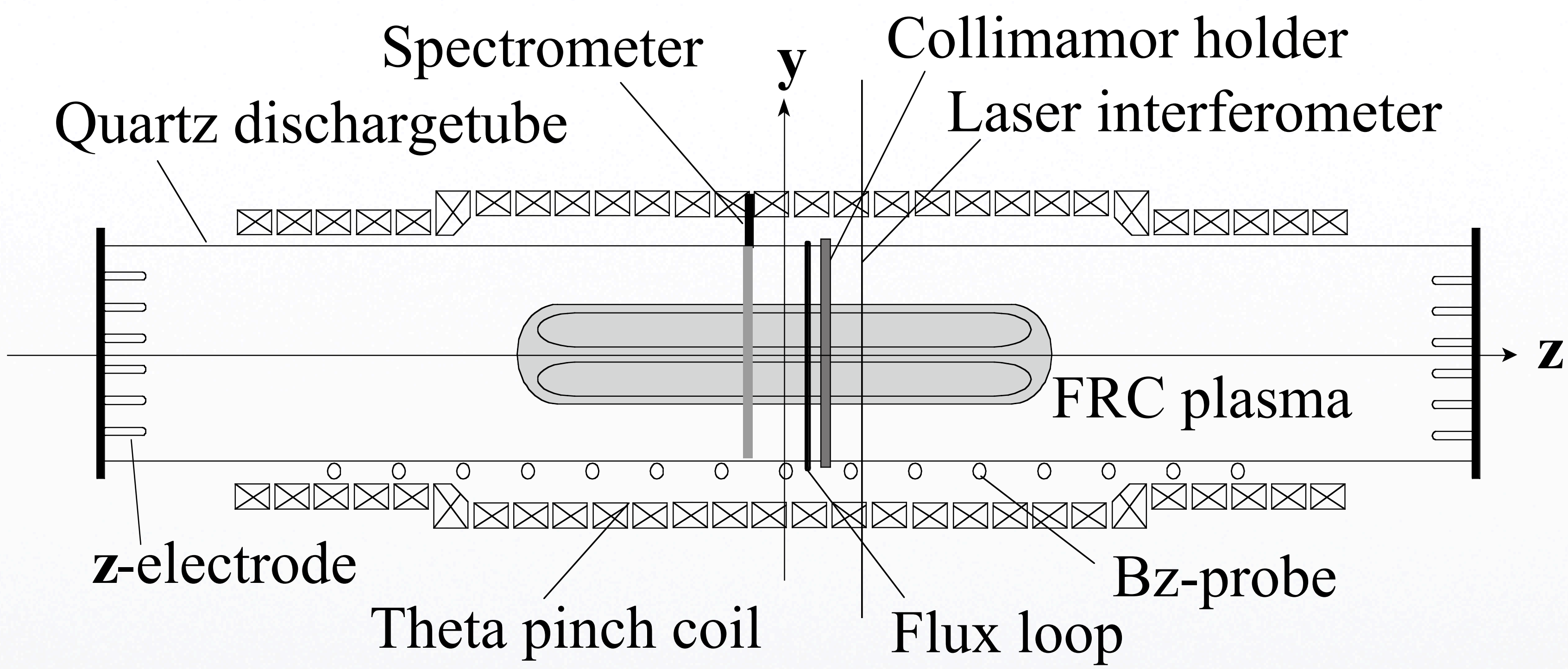

The FRC plasmas were generated on the NUCTE -III device . The central part of the theta pinch coil is 0.9 m in length and 0.34 m in inner diameter. A passive mirror coil of axial length 0.3 m and 0.3m inner diameter is mounted at each end. These coils provide an on-axis vacuum mirror ratio of 1.23. The theta pinch coil is connected with a 5 kV, 1.92 mF of capacitor bank and a 32 kV, 67.5 μF fast capacitor bank. The transparent synthetic silica tube, 2 m in length and 0.256m in diameter, is employed as a discharge chamber.

Operation of NUCTE III

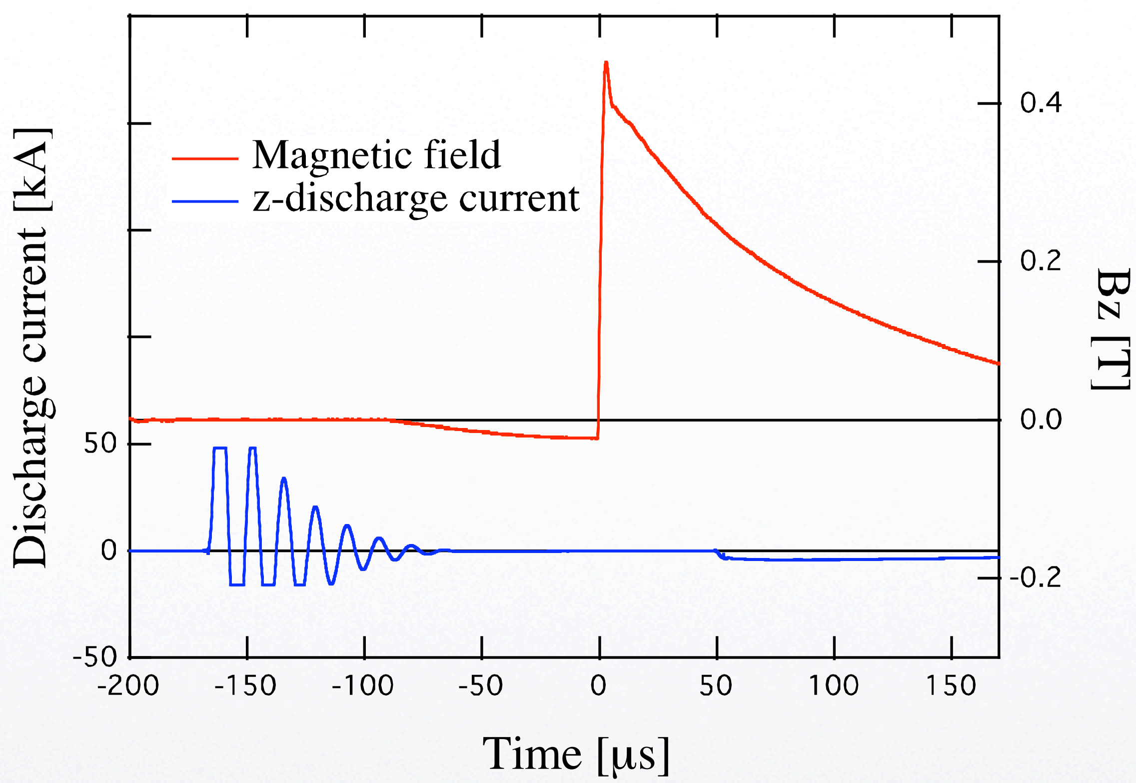

Typical time histories of operation waves are shown in figure. In this device, FRCs are formed by a typical field-reversed theta-pinch method with z-discharge preheating.

In the standard operation case, the main reversed field is provided at the peak of the bias field.

Typical Plasma Parameters

Plasma parameter - Standard operation	
Filling pressure	**10 [mTorr]**
Bias field	**0.032 [T]**
Confinement field	**0.50 [T]**
Separatrix radius	**0.060 [m]**
Separatrix length	**0.8 [m]**
Electron density	**2.5 [x10 /m]**
Total temperature	**270 [eV]**
Particle confinement time	**80 [μs]**

The diagnostics for measuring typical plasma parameters consist of a helium-neon interferometer to measure line-integrated electron density and a flux loop with a set of magnetic probes to determine an axial profile of separatrix radius $r_s(z)$ using the excluded flux method. Here, average electron density is estimated as $\int ndl/2r_s$.

Bremsstrahlung

In this set of experiments, the wavelength was selected by a band-pass inter-ference filter with a central wavelength of 550 nm and bandwidth of 10 nm to avoid impurities and deuterium line spectra. Therefore, only bremsstrahlung (and possibly negligible recombination radiation) is detected by the PMTs. The wavelength dependence of bremsstrahlung can be written as

$$I(\lambda)d\lambda = \propto n_e^2 Z_{eff} T_e^{1/2} \frac{c}{\lambda^2} \exp\left(-\frac{hc}{\lambda T_e}\right) \bar{g}_s d\lambda$$

where Zeff is effective charge number, Te: electron temperature, c: velocity of light, λ: wavelength, h: Planck's constant and g s is the Gaunt factor. For these experimental conditions, the exponential term can be approximated as unity; therefore the intensity I(λ) becomes

$$I(\lambda)d\lambda = \propto n_e^2 Z_{eff} T_e^{-1/2} \frac{c}{\lambda^2} \bar{g}_s d\lambda$$

Computer Tomography

CT(Computer tomography) is the reconstruction task that estimates a two or three dimensional image or profile of the objection from a lot of the projections of the objection at various directions.

If the objection is time-stationary like a human body, all the projection of the objection can be obtained by a scanning the detector system.

But When the objection changes with time and without the good reproducibility like plasma diagnostic, many detectors must be fixed around the objection to obtained the time resolved projections.

In our experiments, arrengeble and flexible optical diagnostic system which consists of multichannel detectors has been developed to observed the time history of the toroidal cross section of the FRC plasma.

CT (ART method)

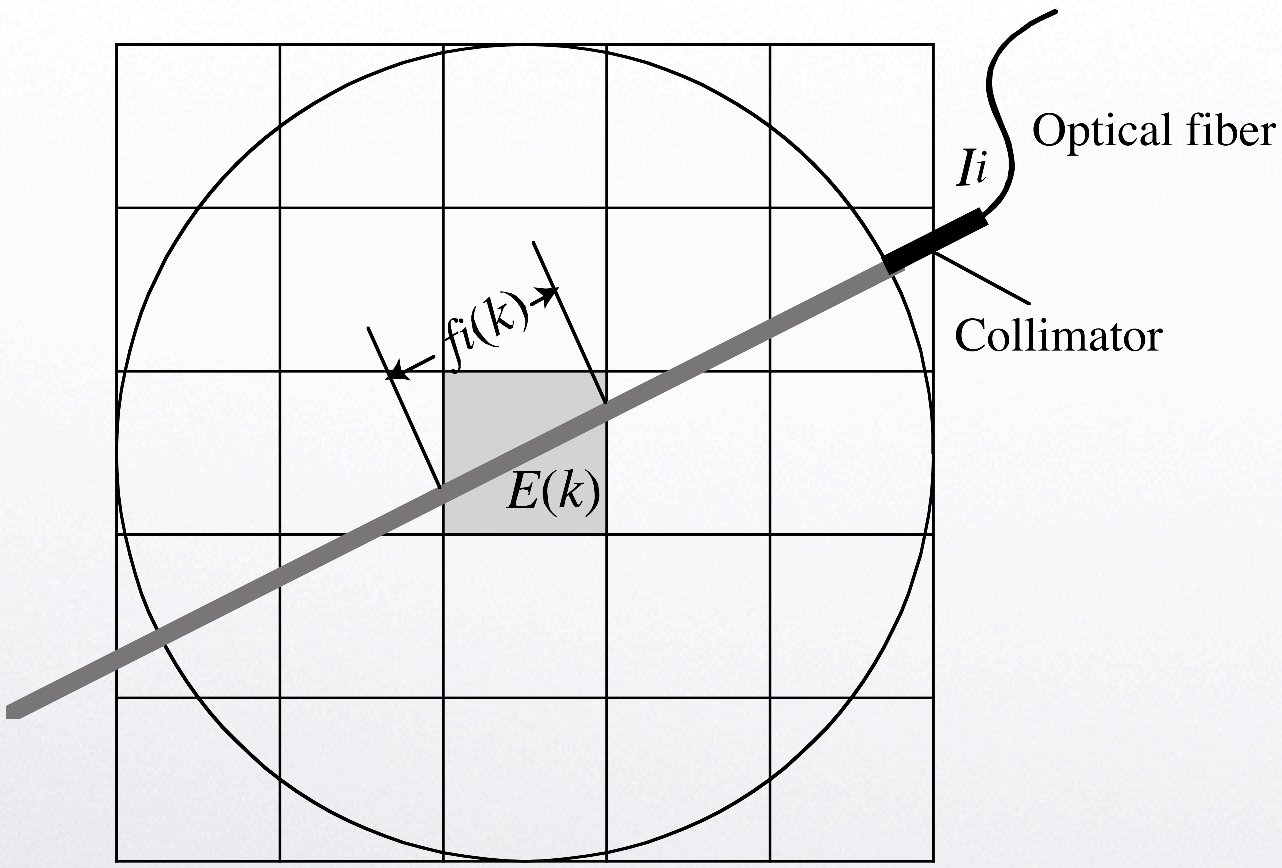

ART method can reconstruct without an assumption of a symmetry of an observed plasma. The collimator observes the line integrated light intensity along its optical axis.

$$I_i = \int_{Li} \varepsilon(r, \theta) dl$$

In ART method, the region of reconstruction is divided into the small cell. $\varepsilon(r,\theta)$ is represented as $E(k)$ (k=1,....k_m). k_m is the number of the cell

$$I_i = \sum_k f_i(k) E(k)$$

$f_i(k)$ is weight function which represents the length across the cell by the optical axis.

Computer Tomography (ART)

weight function **projection data** **emissivity**

$$F = \begin{pmatrix} f_{1_m}(1) & \dots & f_{1_m}(k_m) \\ \vdots & \ddots & \vdots \\ f_{i_m}(1) & \dots & f_{i_m}(k_m) \end{pmatrix}, \quad I = \begin{pmatrix} f_{1_m} \\ \vdots \\ f_{i_m} \end{pmatrix}, \quad E = \begin{pmatrix} f_{1_m} \\ \vdots \\ f_{k_m} \end{pmatrix}$$

$$I = F \cdot E \qquad (i_m \geq k_m)$$

Solution of E is obtained by the least square solution

$$E = (F^t \cdot F)^{-1} \cdot F^t \cdot I$$

E is solved by the iterative method

$$E^{(l+1)} = E^{(l)} + dq^{(l)}$$

$$dq^{(l)} = F^t(I^F \cdot E^{(l)})$$

Collimators Alignment (Azimuthal Array)

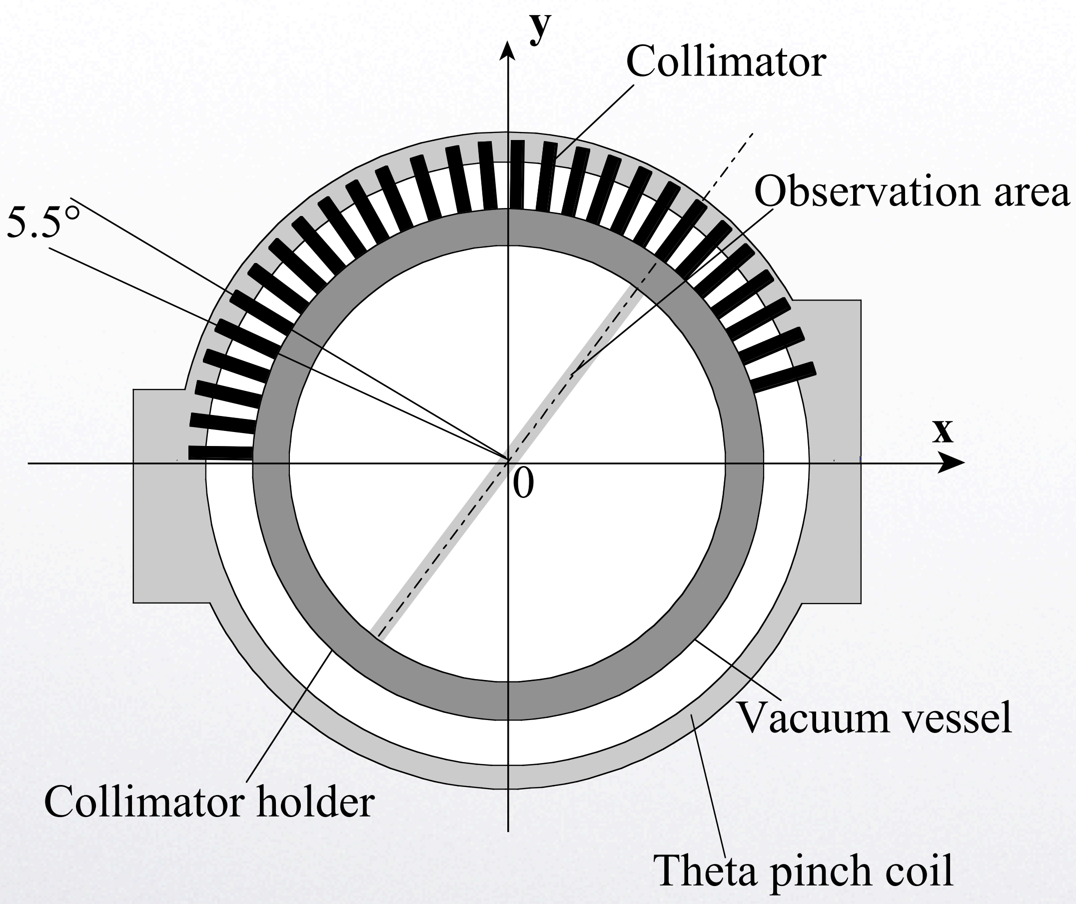

The spatial resolution of the collimator may approximate with ϕ 6mm And the divergence of the light is roughly 0.0025rad.

In the azimuthal holder shown in Figure, all collimators aim to the center of device and arrange to the azumuthal direction at every 5.5°.

Collimators Alignment (CT)

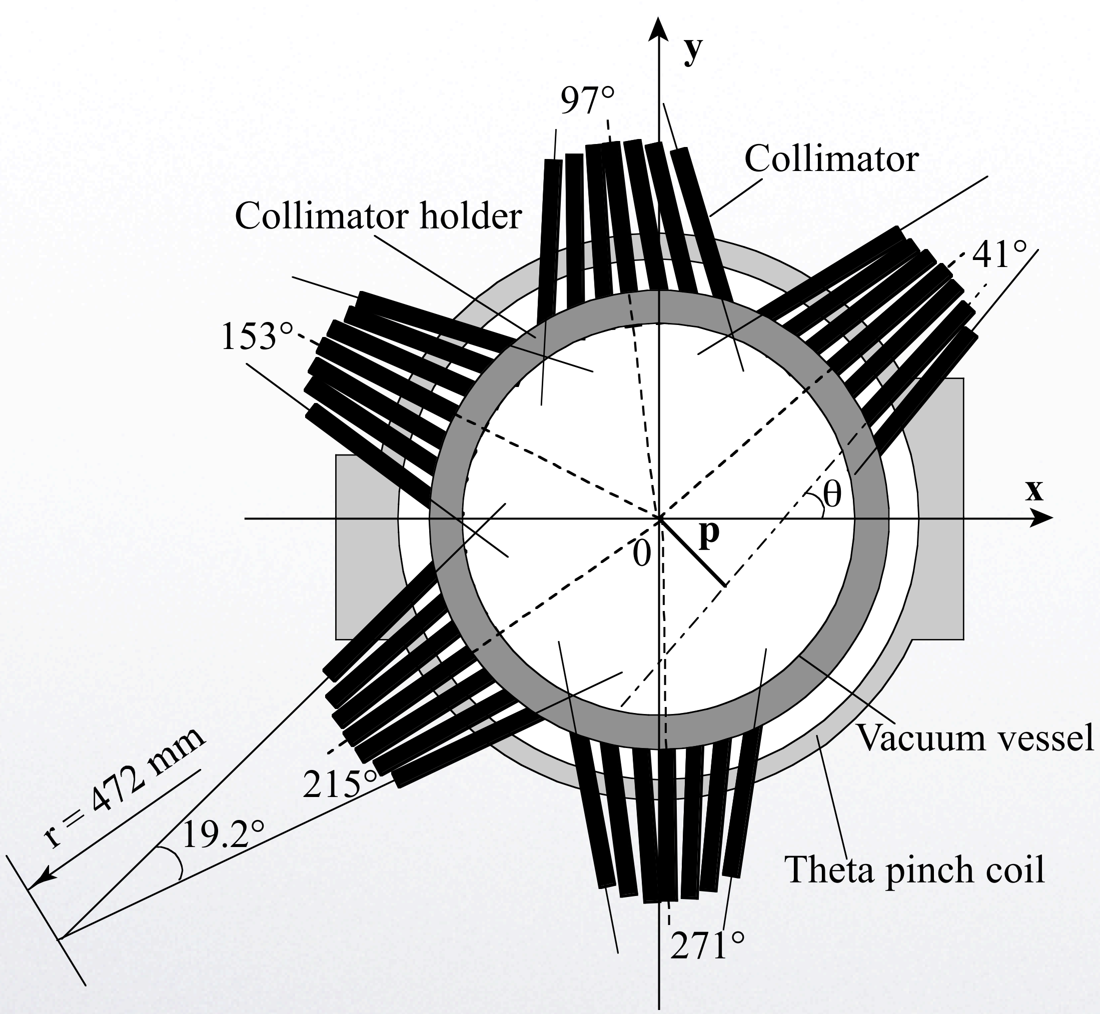

The thirty-five collimators fixed to a holder shown in figure are arranged at z=5.5cm. This holder is consisted of five fan arrays. Relative fan angles are 41^o, 97^o, 153^o, 215^o and 271^o and seven collimators are installed on each fan from -9.6^o to 9.6^o with the same interval angle.

p-θ diagram of the collimator position

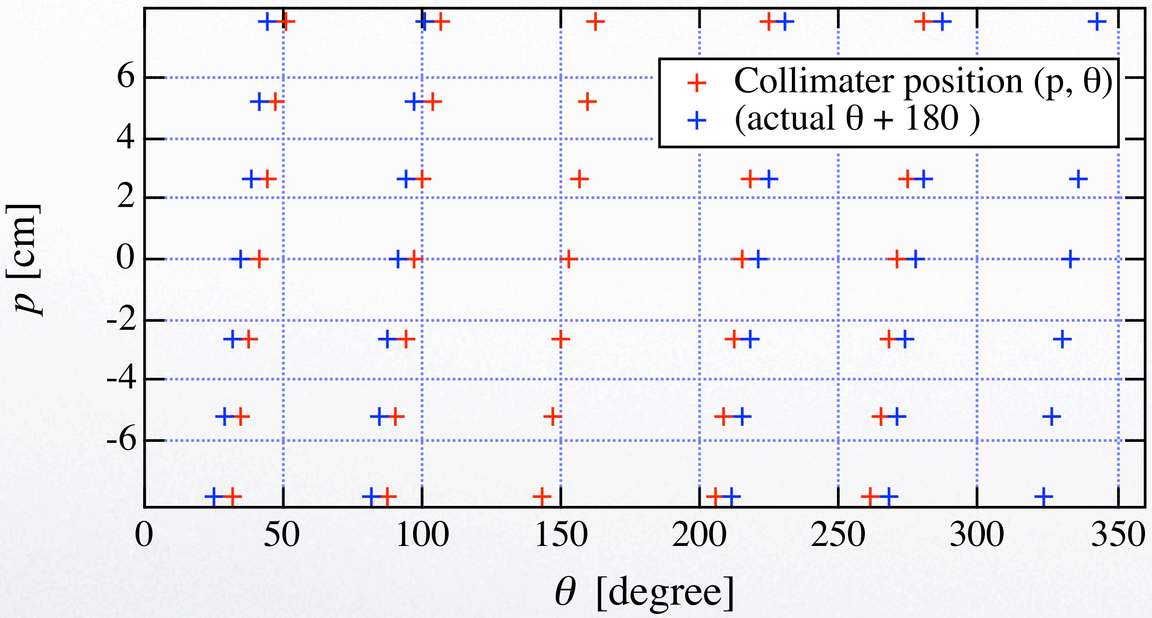

This figure indicates p-θ diagram of the collimator position for CT, where p is a distance of a sight line of the collimator from the center of device and θ is an angle between the sight line and x axis. Red markers are actual positions. Blue markers are (actual θ) + 180° positions. There are measuring line-integrated intensity, so it observe even a blue position at the same time. By sampling theorem, the decidable maximum deformation toroidal mode number that can be observed in this system is n = 4, because the measured data set has ten sets of information relating to the azimuthal direction.

Conclusion of CT

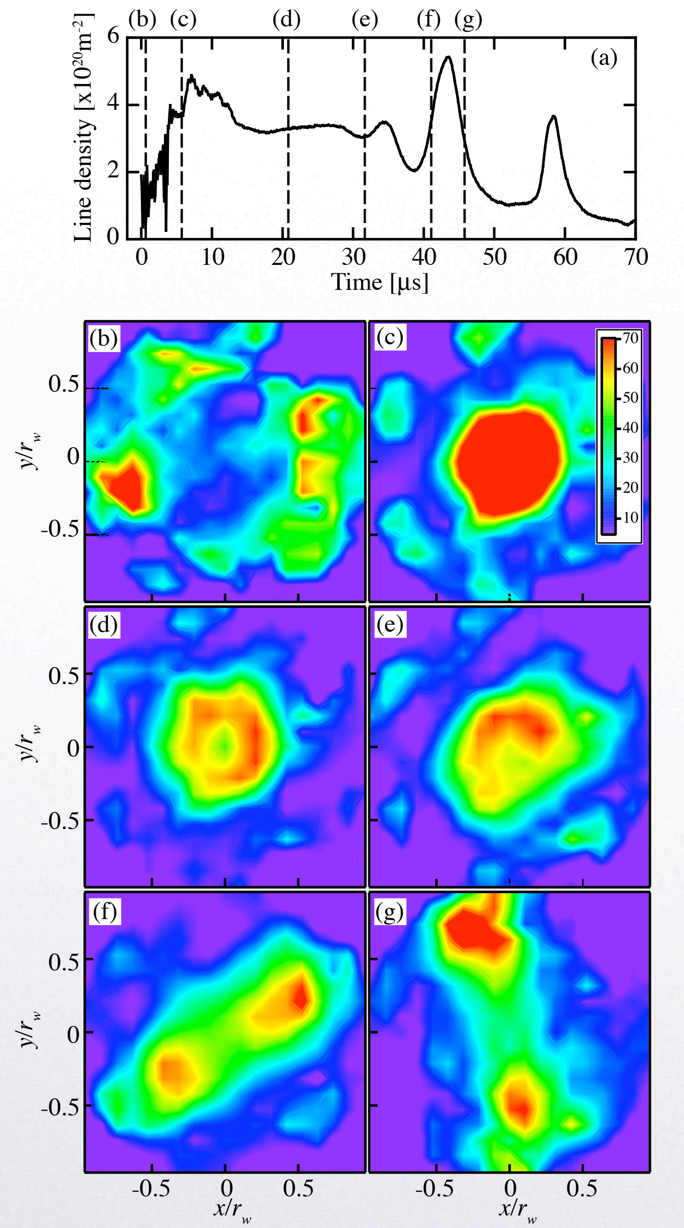

Figure (a) shows time evolution of line integrated electron density $\int n dl$ along the y axis.

In the latter phase of equilibrium, an FRC has a well-known global rotational instability with toroidal mode number n = 2. It has been believed that elliptical deformation of the FRC allows interaction between the wall and the plasma, which terminates this configuration.

However, these experiments revealed the FRC to deform into a dumbbell-like structure before the edge hits the chamber wall, leading to the disruption phase. In addition, an internal shift toroidal mode number n = 1 mode was observed in the equilibrium phase, followed by growth of n = 2 rotational instability.

Mode analysis

Toroidal mode of FRC plasma is defined as fallow,

$$r(\theta) = \int_0^\infty r_n \sin(n\theta + \varphi_n) dn \, .$$

r(θ) : plasm radius
r_n : amplitude of mode
Φ_n : Phase of mode
n : torodal mode number

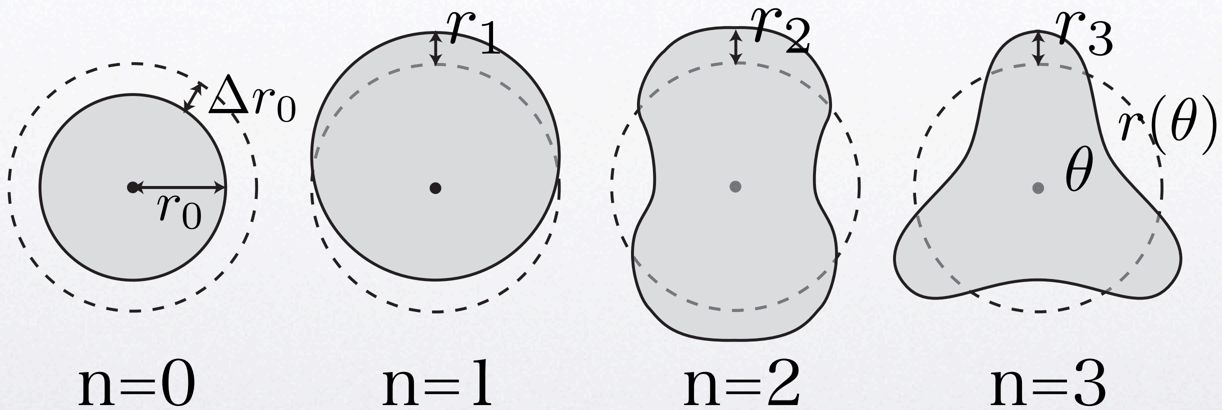

Deformation by the mode of low-level

Method of deciding a boundary

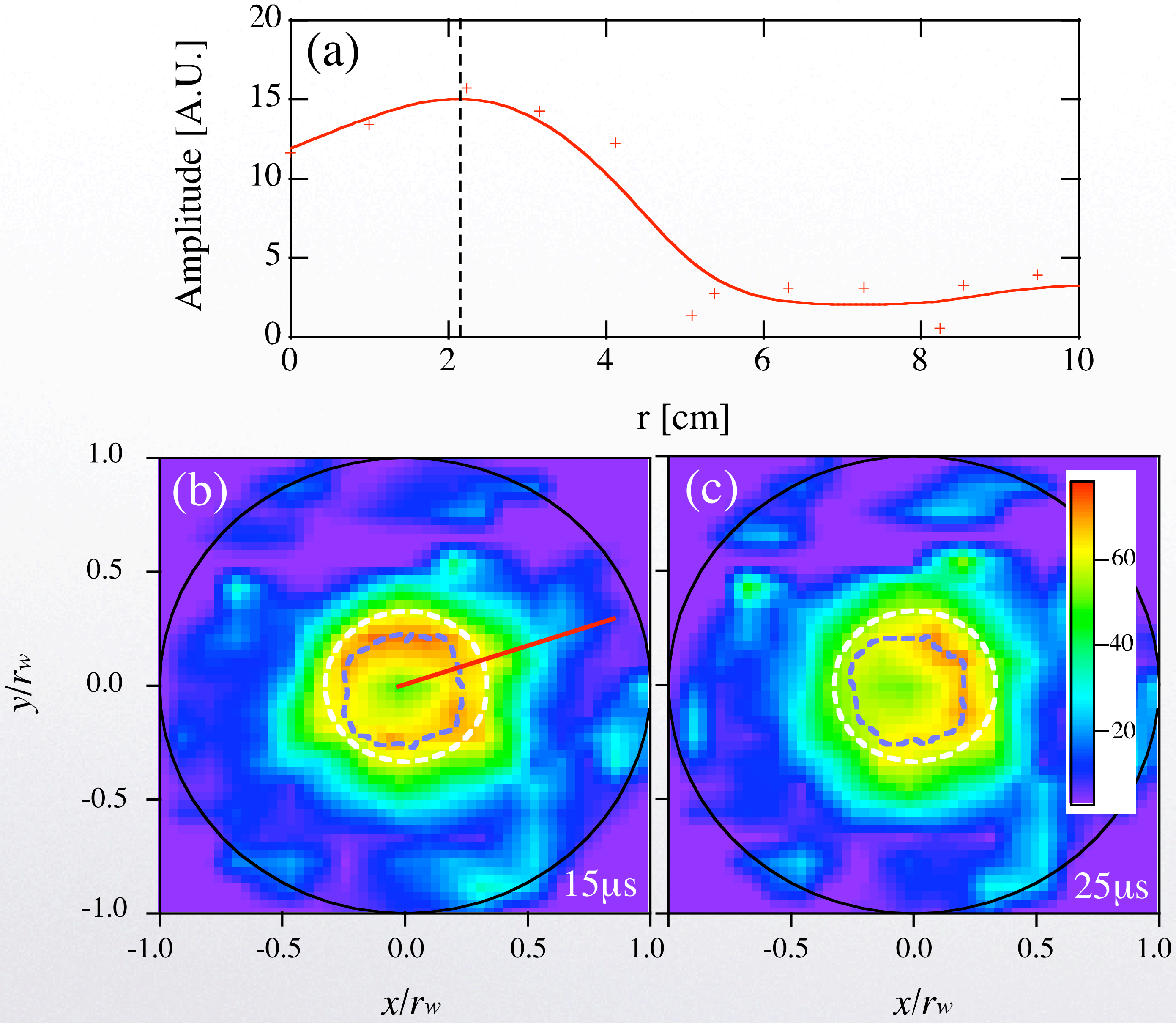

Figure (a) shows amplitude of CT image along the radial axis (red line of figure (b)). (b) and (c) draw tomographic profile of toroidal cross section at 15 and 25μs, respectively. White dashed line in the drawing indicates separatrix estimated by excluded flux method. Blue dashed line in the drawing is the boundary which defined by connecting each radial peak.

Figure (c), An internal shift toroidal mode number n = 1 mode was observed in the equilibrium phase.

Mode analysis (Amplitude)

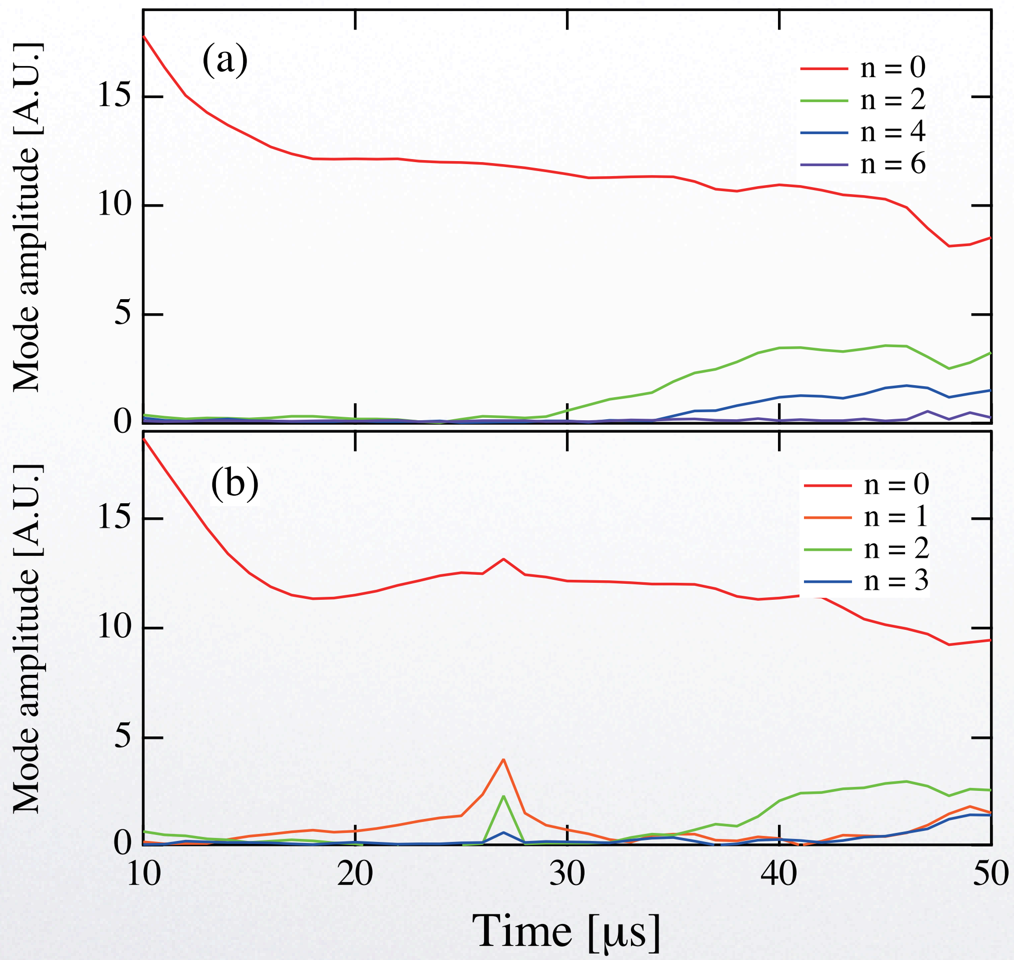

(a) shows time evolution of toroidal mode amplitude calculated from the line integrated emission intensity observed by azimuthally arranged optical collimators In this observation, only even number of toroidal mode can be estimated. This analysis shows no growth of mode amplitude in the toroidal mode number greater than 4.

(b) whole reconstructed area of tomographic profile. Curves of mode number n = 0 and 2 has similarity shape with the results from line integrated measurement (b). This also indicates confidence of the reconstruction.

Mode analysis (Amplitude)

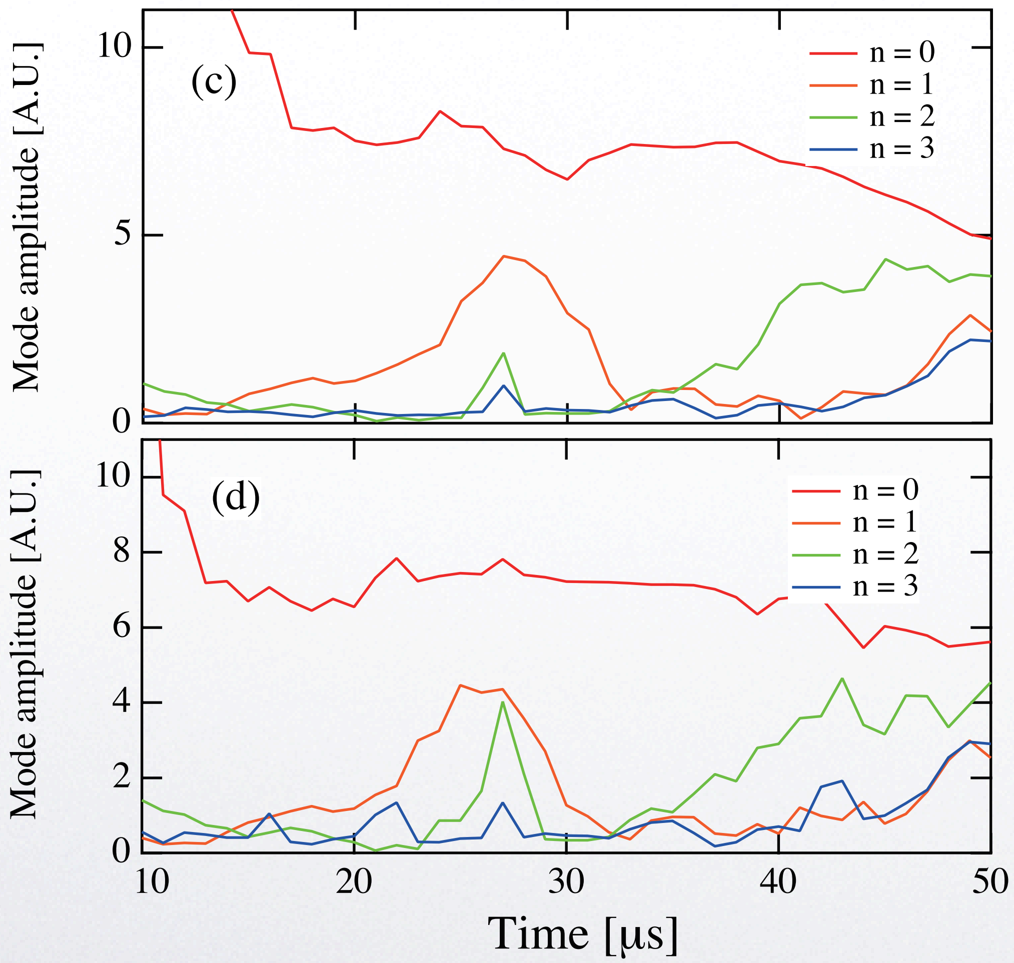

Time evolution of toroidal mode amplitude analyzed from (c) inside the separatrix, (d) inside the boundary which defined by connecting each radial peak.
Even in the quiescent phase of time history of $\int n dl$, these tomographic profiles show deformation of cross section. At 15μs , irregularity of the emissivity on the θ direction is small and illustrates good equilibrium profile. However (c), (d) shows deformed emissive profile especially inside the separatrix even in the flat $\int n dl$ phase.

Summary

The detailed aspect of internal structure is veiled in the usual line integrated diagnostics in a FRC and tomographic technique is useful in confirming the diagnosis of internal toroidal mode deformation as well as that of external mode.

Tomographic profile of presented method has detected toroidal mode deformation especially inside the separatrix. However, it is difficult to investigate time evolution of internal structure, especially around the magnetic axis (a null point), with the spatial resolution of presented system. Thus, for more detailed investigation, improvement of spatial resolution by adding measurement points or improvement reconstruction technique for example optimization of the weight of divided cells are necessary as far as an information theory permits it.